

Article

A Comparison of the Microbial Community and Functional Genes Present in Free-Living and Soil Particle-Attached Bacteria from an Aerobic Bioslurry Reactor Treating High-Molecular-Weight PAHs

Chu-Chun Yu ¹, Ting-Chieh Chang ¹, Chien-Sen Liao ²  and Yi-Tang Chang ^{1,*} 

¹ Department of Microbiology, Soochow University, Shilin District, Taipei 11102, Taiwan; dorisyu10231@gmail.com (C.-C.Y.); jtjuuu0427@gmail.com (T.-C.C.)

² Department of Civil and Ecological Engineering, I Shou University, Kaohsiung 84001, Taiwan; csliao@isu.edu.tw

* Correspondence: ytchang@scu.edu.tw; Tel.: +886-2-28819471 (ext. 6862)

Received: 27 January 2019; Accepted: 12 February 2019; Published: 19 February 2019



Abstract: High-molecular-weight (HMW) polycyclic aromatic hydrocarbons (PAHs) contaminate a wide range of ecosystems, including soils, groundwater, rivers and harbor sediments. The effective removal of HMW PAHs is a difficult challenge if a rapid remediation time and low economic cost are required. Bioremediation provides a cheap and eco-friendly cleanup strategy for the removal of HMW PAHs. Previous studies have focused on removal efficiency during PAHs bioremediation. In such studies, only limited research has targeted the bacterial communities and functional genes present in such bioremediation systems, specifically those of free-living (aqueous) bacteria and soil particle-attached bacteria present. In this study, a high-level of HMW PAH (1992 mg/kg pyrene) was bioremediated in an aerobic bioslurry reactor (ABR) for 42 days. The results showed a pseudo first order constant rate for pyrene biodegradation of 0.0696 day⁻¹. The microbial communities forming free-living bacteria and soil-attached bacteria in the ABR were found to be different. An analysis of the aqueous samples identified free-living *Mycobacterium* spp., *Pseudomonas putida*, *Rhodanobacter* spp. and *Burkholderia* spp.; these organisms would seem to be involved in pyrene biodegradation. Various biointermediates, including phenanthrene, catechol, dibenzothiophene, 4,4'-bipyrimidine and cyclopentaphenanthrene, were identified and measured in the aqueous samples. When a similar approach was taken with the soil particle samples, most of the attached bacterial species did not seem to be involved in pyrene biodegradation. Furthermore, community level physiological profiling resulted in significantly different results for the aqueous and soil particle samples. Nevertheless, these two bacterial populations both showed positive signals for the presence of various dioxygenases, including PAHs-RHD α dioxygenases, riesk iron-sulfur motif dioxygenases and catechol 2,3-dioxygenases. The present findings provide a foundation that should help environmental engineers when designing future HMW PAH bioremediation systems that use the ABR approach.

Keywords: PAHs; free-living bacteria; soil particle-attached bacteria; community level physiological profiling; dioxygenases

1. Introduction

PAHs are common fused benzene ring pollutants that are generated in large amounts when an incomplete combustion process occurs during a variety of industrial activities, when there is uncontrolled burning of waste and fossil fuels and during forest fires. Examples of PAH-generating industrial activities include the production of various chemicals, such as creosote, wood preservatives,

coal tar and various other coal and oil derivatives [1]. High molecular weight (HMW) PAHs are defined as chemicals that have the structure of a PAH and consist of more than three aromatic benzene rings. In Taiwan, many HMW PAHs are USEPA 16 PAH priority pollutants; they are found in many petroleum hydrocarbons contaminated soils and in groundwater. HMW PAHs are toxic and are considered to be carcinogenic, mutagenic and teratogenic pollutants that pose a serious threat to both human health and the health of the ecological environment. The low water solubility (S_w) of HMW PAHs limits their bioavailability in the natural environment. Effective remediation technologies are urgently required that are able to carry out either in-situ or ex-situ treatment that is able to bring about the mineralization of HMW PAHs. Bioremediation provides an economic and eco-friendly cleanup strategy for HMW PAHs removal. Aerobic bioslurry reactors (ABRs) have been reported to remediate high levels of persistent organic pollutants (POPs) in contaminated soils at a lower viscosity using a soil/water system. The effective removal of POPs can be carried out via the complete mixing that occurs in an ABR; in such circumstances, insecticides, PCBs, TPHs, PAHs and similar chemicals have been shown to be biomineralized [2–5]. To obtain the best performance in terms of POPs bioremediation, each system needs to be operated at its optimal parameters; these include pH, temperature, dissolved oxygen (DO), the soil/water ratio of the system and even the stirring speed of the ABR [6].

The effective removal of HMW PAHs using ABRs has been widely reported in previous studies. Bacterial community analysis of these ABRs has focused on the species that seem to be involved in the microbial biodegradation of the HMW PAHs [7]. Nevertheless, there is little information available on the different bacterial communities present in the ABRs, such as the physiological characteristics of free-living and soil particle-attached bacteria present during the biodegradation of the HMW PAHs in the ABR. Specifically, although comparative analyses of free-living (aqueous) bacteria and soil particle-attached bacteria present in the soil/water systems have been reported for a number of natural environments, few studies have examined them during POPs bioremediation in an ABR. In general, free-living bacteria identified in such soil/water systems have been found to have excellent biodegrading abilities with respect to the HMW PAHs present in the aqueous phase. By way of contrast, soil particle-attached bacteria in such soil/water systems seem to only provide some indirect assistance with respect to HMW PAHs biodegradation. Such assistance, for example, includes the formation of bacterial biofilms on the soil particles and the development of relevant microbial ecological cycles [8,9]. Based on the above-mentioned mechanisms, it seems likely that the rate of mass transfer of HMW PAHs from attached-soil particle status to aqueous status plays an important role in the functioning of the ABR system. A higher HMW PAH K_{ow} value means there will be a lower bioavailability of HMW PAH in the ABR due to there being restricted mass diffusion within the complicated soil slurry matrix [4,10]. However, the hydrological and geological characteristics of fractured rock aquifers will also affect the contribution of free-living bacteria and soil particle-attached bacteria. For example, free-living bacteria indigenous to a karst aquifer has been described as not being suited for natural bioremediation because of the small microbial contribution of these bacteria during the toluene biodegradation process compared to the contribution of the attached bacteria [11]. These findings suggest that the contribution of free-living bacteria during POPs bioremediation is likely to vary on a case-by-case when different soil/water systems are explored.

The objective in this study is to compare the differences between bacterial communities when biodegrading a target HMW PAH, namely pyrene (PYR), in an ABR. Microbial diversity assessments and community-level physiological profiling (CLPP) during the PYR bioremediation were used to clarify the differences between free-living bacteria and soil-particle attached bacteria present in the reactor. In addition, we also identify and discuss the relationships between biometabolites and their chemical functional groups. These experimental results provide important practical information regarding the roles of free-living bacteria and soil particle-attached bacteria in an ABR system and this will help in the future with the development of more effective POPs bioremediation systems using the ABR approach.

2. Materials and Methods

2.1. PAH, Soil, Microorganisms, Chemicals

PYR was purchased from the Aldrich Chemical Company (>99% purity) and this was used as the target HMW PAH. A Tapumei series (Tf) red soil, which was obtained from Mingen Village, Nai-tuo County, in central Taiwan (N 23°86'97.22", E 120°61'58.57"), was used in the experiments. Before the experiments commenced, the Tf soil samples were air-dried and then sieved to obtain particles of less than 2.00 mm. The soil characteristics were then analyzed and are listed in Table 1. The soil was classified as a clay loam (CL) based on U.S. Soil Taxonomy. A stimulated PYR-contaminated soil was used to model a typical HMW PAH-contaminated soil in these experiments. The PYR stock solution, prepared by dissolved 0.2 g PYR in 100 mL acetone, was added to 1000 g of dry Tf soil. The resulting soil sample was subjected to complete mixing at 200 rpm for 16 h and then was placed in a chemical hood to allow the complete evaporation of the acetone. This PYR-contaminated Tf soil (theoretically at a level of 2000 mg kg⁻¹) was used throughout these experiments.

Table 1. The properties of the Tf red soil.

Soil	Composition (%)			pH	CEC ¹ (cmol/kg)	SOM ² (%)	Total Fe (%)
	Sand	Silt	Clay				
Tf	51.0 ± 0.2	4.0 ± 0.3	45.0 ± 0.5	4.80 ± 0.12	14.1 ± 0.2	1.8 ± 0.1	3.35 ± 0.22

¹ cation exchange capacity; ² soil organic matter.

PYR-biodegraders are present in PAH-contaminated soils in Taiwan and these organisms had been enriched previously via a series of batch cultures by incubation in a chemostat system as described earlier [8]. The substrates fed into the above chemostat (this is called chemostat N in this paper) consisted of three PAHs (naphthalene, phenanthrene and PYR); these acted as carbon sources. These carbon sources were available at their theoretical S_w values and had been added to the mineral basal medium (MSB), which has the composition 100 mg L⁻¹ CaCl₂, 10 mg L⁻¹ FeCl₃, 100 mg L⁻¹ MgSO₄·7H₂O, 100 mg L⁻¹ NH₄NO₃, 200 mg L⁻¹ KH₂PO₄ and 800 mg L⁻¹ K₂HPO₄. After enrichment, a 500 mL inoculum was transferred from the chemostat N into the batch reactor; the batch reactor contained MSB and PYR as sole carbon source at the concentration outlined below. Every two weeks 1500 mL of fresh MSB containing 2000 mg L⁻¹ of PYR were added to the batch reactor and, at the same time, 1500 mL of liquid was discarded; this was in order to keep the volume of medium in the reactor constant throughout the biodegradation experiments (this is called N2000 in this paper). The bacteria present in the batch reactor have been shown to have the ability to carry out PYR biodegradation before these experiments began (unpublished data). Double-deionized water (>18 MΩcm) was used for all aqueous solutions and dilutions, and this was obtained from a Milli-Q deionizing system. All of the chemical reagents and solvents used in this paper were of analytical grade or better, with purities ≥95%.

2.2. HMW PAH Biodegradation Experiments in the ABR

A 5L tempered-glass circular ABR (inner diameter 16 cm × height 30 cm) was set up with a PTFE-stir mixer (Global Lab[®], Korea) in these experiments. The experiments initially combined a mixture of 4L of PYR-contaminated bioslurry (the soil/water system) and the PYR-biodegrading organisms within the ABR. The initial bacterial inoculum of PYR-biodegraders from the batch reactor was introduced into the ABR such that the initial bacterial density was 3.19 × 10⁴ CFU mL⁻¹ (about 0.02 optical density at 590 nm). The soil/water ratio of the 4L PYR-contaminated bioslurry in the ABR was set at 2.0 mL aqueous substrate (MSB) to 1.0 g PYR-contaminated Tf soil. The experiments were executed at room temperature (on average this was 26.7 °C during the experiment) and lasted for 42 days. Mixing was complete because there was stirring at 200 rpm by the mixer and this also

created a high DO (on average 8.35 mg L^{-1} in the experiments), which meant that the ABR system was aerobic. A control ABR system was set up under exactly the same conditions as above except that 1% NaN_3 was added to the medium in the ABR. Triplicates for each sample obtained from the ABR were analyzed by following the various analytical methods described below.

2.3. Analytical Methods

2.3.1. The Concentration of PYR

Samples were removed from the two ABRs and extracted using HPLC-grade dichloromethane (CH_2Cl_2). These extracts were injected into an HPLC/UV system (YL-9100, Korea) in order to measure the concentration of PYR in the reactor. Each sample before injection was centrifuged at 4°C and 12,000 rpm for 40 min and then filtered through a $0.22 \mu\text{m}$ PTFE membrane (Millipore Millex[®]) to separate each sample into an aqueous sample (NW) and a soil particle-adsorbed sample (SW). The total concentration of PYR in each ABR system consisted of the aqueous and soil-adsorbed sample values added together. No obvious PYR losses occurred during the equilibration process. A recovery range of 90% to 95% for the amount of PYR present in the equilibrated substrates was obtained; this was a result of analytical errors and the memory effect of the HPLC system after with the passage of PYR. The detection limit for PYR using this approach is 0.1 mg L^{-1} . The conditions used for the HPLC were as follows: ODS C18 Hypersil column (Thermo Scientific[®], 150 mm length, 4.6 mm inner diameter), a 90/10 ratio of methanol/water and absorbance measurement at 285 nm. The retention time of PYR was measured to be 7 min 30s using this HPLC chromatography system.

2.3.2. Biometabolite Analysis by Gas Chromatography–Mass Spectrometry (GC-MS)

The aerobic biometabolites of PYR biodegradation present in the ABR systems were detected by the GC/MS (Agilent 6890N/5975B insert MSD, USA). The column used was a capillary DB-5HT (Agilent, USA). The carrier gas was helium with the 99.999% purity at a rate of 1.0 mL min^{-1} . The temperature program is setup for 20.5 min, under the following conditions: 50°C for an initial 3 min, rising from 50°C to 300°C a speed of $20^\circ\text{C min}^{-1}$ and then the system was kept at 300°C for the last 5 min. The acquisition mode of the MS used was the full scan mode and was at 50–800 amu. The detector temperature and electron impact (EI) mode were 320°C and 69.9 eV, respectively. The m/z profiles of the byproducts were identified using the GC/MS spectra databases NIST 05, Wiley275 and Wiley7n. For the GC/MS analysis, purer extracts were required and an extra cleaning process was introduced that involved a glass chromatography column packed with acidic silica gel. In order to prepare the acidic silica gel, 60–200 mesh neutral silica gel (Merck, Darmstadt, Germany) was added to 40% concentrated sulfuric acid (w/w) and kept at 130°C for 16 h. The sample extract was eluted from the acidic silica gel column using 20 mL hexane and then concentrated to near dryness by rotary evaporation. Finally, the remaining residues were dissolved in a rotary evaporation flask to give a final volume of 1 mL hexane and then filtered through a $0.20 \mu\text{m}$ PTFE syringe filter before being used for the chromatographic analysis.

2.3.3. Detection of the Functional Groups of the Biometabolites Analysis by FTIR

The chemical functional groups of the biometabolites will change as PYR biodegradation proceeds in the ABR and this was monitored by FTIR spectroscopy. The FTIR profile is able to identify the functional chemical bonds present in possible GC-MS metabolites. The samples were initially separated into NW and SW as previously described. The NW samples (5 mL) were then mixed completely with KBr and dried at 105°C oven until the sample had the appearance of a white crystal powder. These white dry powder samples were then ground into fine particles and stored in brown serums until FTIR analysis was carried out. FTIR analysis was carried out on a Shimadzu IR Prestige 21 with using attenuated total reflection (Specac Goldengate). Changes in % transmission at different wavelengths were collected. The FTIR analysis of the extracted biometabolites was compared with the

results obtained from the NW of the PYR-contaminated Tf soil/water system (the ABR control system) using the mid IR region of 400–4,000 cm^{-1} with a scan speed of 16.

2.3.4. Bacterial Community Analysis

1. Obtaining samples of free-living bacteria and soil particle-attached bacteria

Samples (30 mL soil/water) obtained from the PYR biodegradation system in the ABR were centrifuged at 500 rpm, 25 °C, for 2 min then 10 mL of the aqueous solution was discarded. The remaining 20 mL of soil/water sample was then centrifuged again at 5000 rpm, 25 °C for 20 min to separate the sample into an aqueous sample and a soil-particle sample. The aqueous samples containing free-living bacteria (7.5 mL) were mixed completely with 12.5 mL 0.85% NaCl. The soil particle-attached bacteria samples were then centrifuged down again at 5000 rpm, 25 °C for 20 min and then pellet completely mixed with 20 mL of 0.85% NaCl.

2. Biodiversity assessment by the DGGE method

Genomic DNAs from the samples of free-living bacteria and the soil particle-attached bacteria involved in PYR bioremediation were extracted using a soil genomic DNA purification kit (Gene Mark, Taiwan). The p63f-GC/p2 primers (forward primer p63f (5'-CAGGCCTAACACATGCAAGTC-3')-GC clamp and reverse primer p2 (5'-ATTACCGCGGCTGCTGG-3')) were used to selectively amplify the V1-V3 regions of 16S rDNAs by polymerase chain reaction (PCR). The DNA products of the PCR were separated by DGGE profiling using the DCode™ Universal Mutation Detection System (Bio-Rad Laboratories, Inc., USA) system and a 35–55% gradient gel at 60 °C and 110 V for 18 h. The acrylamide percentage used for the DGGE electrophoresis gel was 8% and the denaturing agents were formamide and urea. The significant DNA bands, many of which were common across the DGGE profile were extracted from the gel, mixed with 10 μl of sterilized Milli-Q water, and then reamplified using the same p63/p2 primer pair.

3. Cloning to allow bacterial identification

The various amplified rDNAs encompassing the V1-V3 region were purified using an SV Gel followed by purification using a PCR clean up kit (Wizard®, USA). The cleaned-up product was then cloned using a pGEM®-T Easy Vector Systems kit (Promega, Madison, Wisconsin, USA) and transformed into competent *Escherichia coli* DH5 α cells as outlined by the manufacturer. The transformed *E. coli* was incubated on LB agar plates at 37 °C overnight and the next day the blue-white screening method was applied to select all of the white colonies from each population. Plasmid DNA from each colony was then extracted using an EasyPure Plasmid DNA miniprep kit (Bioman, Taiwan). The DNA inserts in each of these plasmids was amplified by PCR using the primers: M13-F (5'-GTT-TTC-CCA-GTC-ACG-AC-3') and M13-R (5'-ACA-GGA-AAC -AGC-TAT-GA-3') and the size checked to confirm the presence of the correct insert. The various 16S rRNA inserts were then sequenced by the National Core Facility Program for Biotechnology at the National Yang-Ming University, Taiwan. All sequences were compared using BLAST against the reference microorganisms contained in the NCBI GenBank database. The closest 16S rDNA sequences to the 16S rRNA sequences obtained from the bacteria making up the biodegradation bacterial populations were retrieved. These sequences, including the new rDNA sequences from the ABR system, were then aligned using Clustal X software.

2.3.5. Targeted Analysis of the Dioxygenase Genes

Genomic DNA of the aqueous samples of free-living bacteria were analyzed to detect the presence of genes encoding the functional dioxygenases that are known to be involved in PYR biodegradation. Since the chemical structure of PYR consists of four aromatic benzene rings, this structure is vulnerable to serial benzene ring-cleavage reactions by dioxygenases under aerobic conditions. Genes encoding dioxygenases are well known to be involved in the aerobic biodegradation

of PYR. Different aromatic benzene rings are able to be cleaved by various dioxygenases; specifically dioxygenases in a number of different bacterial species have been shown to bring about the oxidative cleavage of catechol in particular. Table 2 lists the primer pairs able to detect the four selective functional genes that are likely to be involved in PYR biodegradation by bacteria in this study. The dioxygenases involved are: The PAHs-RHD α (RHD α), ring-hydroxylating dioxygenases (Nid A), the rieske iron-sulfur dioxygenases (Rf), the protocatechuate 3,4-oxygenases (EC 1.3.11.3, C34O) and the catechol 2,3-dioxygenases (EC 1.3.11.2, C23O).

Table 2. PCR primers for the various dioxygenases that were targeted in this study.

Target Gene (Abbreviation)	Primers	Sequence (5'→3')	Size (bp)	Reference
PAHs-RHD α (RHD α)	396F 696R	ATTGCGCTTAYCAYGGBTGG ATAGGTGTCTCCAACRAARTT	320	[12]
Rieske iron-sulfur motif (Rf1)	Rf1 Rr1	AGGGATCCCCANCCRTGRTANSWRCA TGTCCCCGAACCTTGTCCTTC	700	[13]
Protocatechuate 3,4-dioxygenase (P34O)	P34OF P34OR	CTCACGCAGCACGACATCGACCT CCGGGCGCGACTGTCGATCGTGGT	800	[14]
Catechol 2,3-dioxygenase (C23O)	C230F C230R	AAGAGGCATGGGGGCGCACCGGTTTCGATCA CCAGCAAACACCTCGTTGCGGTTGCC	450	[15]
Ring-hydroxylating dioxygenase (Nid A)	NidAf NidAr	ATGACCACCGAAACAACCGAACAGC TCAAGCACGCCCGCCGAATGCGGGAG	1400	[16]

2.3.6. Community Level Performance Profiling (CLPP)

The physiological characterization of the bacterial communities during PYR biodegradation was performed using a Biolog EcoPlateTM (Hayward, CA, USA). The Biolog identification system has been reported to be suitable for the monitoring of microbial communities and the assessment of their functional potential during environmental changes [17,18]. The experimental procedure was executed as described previously [9]. The CLPP was processed by principal component analysis (PCA) based on average well color. The CLPP method consists of the following steps. First, the average well color development (AWCD) is calculated using absorbance values at wavelengths of 590 nm and 700 nm. Second, PCA is performed using the AWCD results and Ward's method. The minimum eigenvalue in the PCA was set to be 0.000 in order to examine all principal component variances. Each point in the CLPP represents a BioLog pattern and the distances between points approximate to the pattern similarities.

3. Results

3.1. PYR Concentration and Biometabolites Analysis in the ABR

Figure 1 shows the PYR biodegradation over time in the ABR. The PYR was removed effectively, with the amount present in the reactor decreasing from 1992 mg kg⁻¹ initially (Day 0) and reaching the compound's detection limit (<0.1 mg kg⁻¹) on Day 42. The removal efficiency of PYR was above 99.99%. The biodegradation rate of a POP usually can be fitted to a pseudo-first-order equation [19]. The pseudo first rate of PYR biodegradation during the present study was calculated to be 0.0696 day⁻¹ (linear regression $r^2 = 0.9504$), which is well above the 0.0192 day⁻¹ obtained in a previous study [20]. Table 3 shows the biometabolites detected during the PYR biodegradation in the ABR. Most of these biometabolites were detected in the NW samples, which suggested that the PYR biodegradation was occurring in the aqueous phase. For example, phenanthrene (96% GC-MS Ident.) and catechol (96% GC-MS Ident.) were detected and identified as PYR biodegradation products in the NW samples only. On the other hand, dibenzothiophene (97% GC-MS Ident.), 4,4'-bipyrimidine (90% GC-MS Ident.), cyclopentaphenanthrene (89% GC-MS Ident.), and 4-Carboxy-5-phenanthrenecarboxaldehyde (91% GC-MS Ident.) were detected and identified in both the NW samples and the SW samples (see the Supplementary, Figure S1). These findings suggest there was a series of biotransformations during PYR

biodegradation that started from PYR and then produced 4-Carboxy-5-phenanthrenecarboxaldehyde, phenanthrene and catechol via a stepwise process.

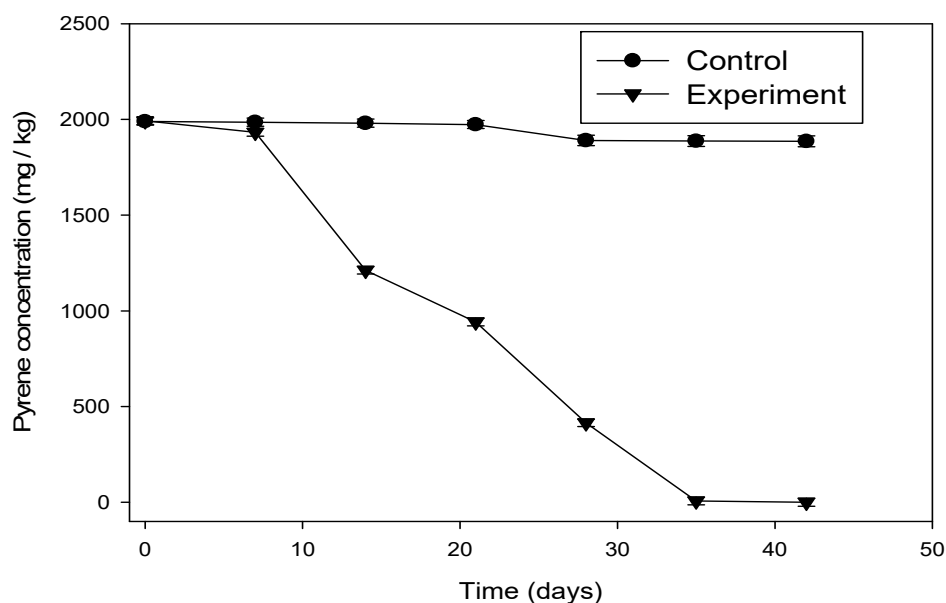


Figure 1. Pyrene (PYR) biodegradation in an aerobic bioslurry reactor (ABR).

Table 3. Biometabolites identified by GC-MS.

Sample ¹	Biometabolites (Identity% by GC-MS)
NW0	ND ²
NS0	
NW2	Phenanthrene (96%), Catechol (96%), Dibenzothiophene (97%), 4,4'-Bipyrimidine (90%), Cyclopentaphenanthrene (89%)
NS2	4-Carboxy-5-phenanthrenecarboxaldehyde (91%)
NW6	Catechol (96%)
NS6	ND ²

¹ NW, aqueous samples; NS, soil particle-attached samples. NW-X and NS-X, where X = 0, 2, 6 presents were the biodegradation samples at 0, 14, 42 days. ² ND, not detected.

Figure 2 shows the FTIR profile of NW samples during PYR biodegradation in the ABR. Significant peaks can be observed that are related to the various chemical bonds within the various functional group present. The following peaks were detected in the PYR-contaminated Tf soil (control): The N-H (stretch)/(bending) of amine ($3100\text{--}3500\text{ cm}^{-1}/1600\text{ cm}^{-1}$); C=C (stretch) of aromatic ($1400\text{--}1700\text{ cm}^{-1}$); C=C (stretch) of alkene ($1620\text{--}1680\text{ cm}^{-1}$); $\text{-(CH}_2\text{)}_2\text{-}$ (bending) (1380 cm^{-1} and 1370 cm^{-1}); C-OH of phenol (1200 cm^{-1}); and C-O (stretch) of ester ($1185\text{--}1200\text{ cm}^{-1}$). These features are known to be present in organic material from soil (such as humin, humus or fulvic acid) and in PYR. Significant variations in the FTIR profile signals (area under the peak) were found for the NW samples. For example, the NW1 sample showed one peak increasing in area within the range $1000\text{--}1300\text{ cm}^{-1}$, which can be assigned to the C-O bonding of alcohols, ethers, carboxylic acids, and esters. Another peak increasing in area was within the range $675\text{--}1000\text{ cm}^{-1}$, which can be assigned to the =C-H (bending) bonding of alkenes. Reducing peak areas within the ranges associated with $\text{-(CH}_2\text{)}_2\text{-}$ (bending) (1380 cm^{-1} and 1370 cm^{-1}) were also detected. These very obvious signals in the NW1 sample finally disappeared in the NW5 and NW6 samples, which indicates the disappearance of these more complex biometabolites as the PYR biodegradation progresses. An increase in peak

area became obvious in the range 3200–3600 cm^{-1} in the NW5 sample. This can be associated with the stretching vibration of hydrogen-bonded alcohols and phenols, which are likely to be the simple biometabolites formed towards the end of the bioremediation process.

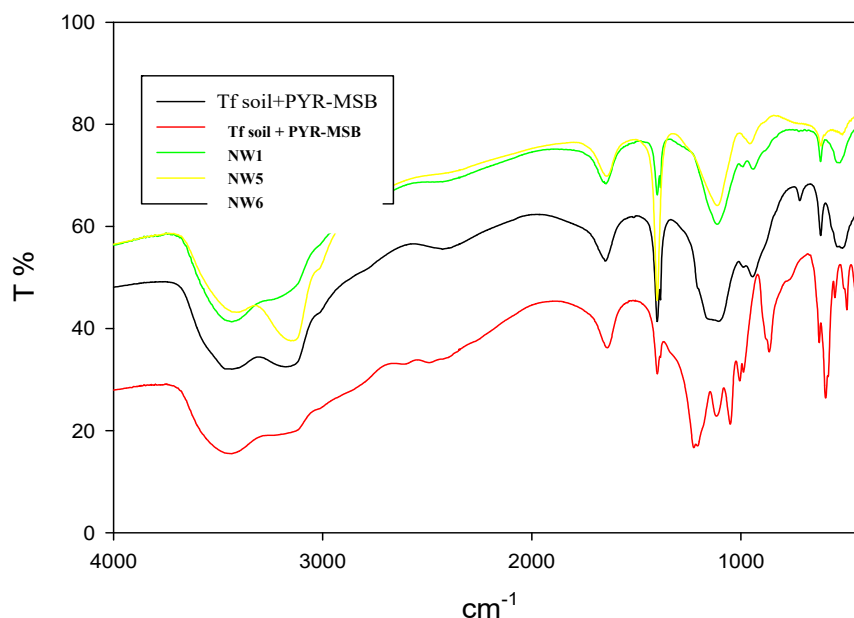


Figure 2. FTIR profiles during the PYR biodegradation in an ABR. No. 1, 5, 6 represent the biodegradation samples at 0, 35, 42 days, respectively.

3.2. Change in the Bacterial Communities as the PYR Biodegradation Progresses in the ABR

Figure 3 shows the fluctuated DGGE profiles of the microbial communities during PYR biodegradation in the ABR. Each band on the DGGE profile represents one bacterial species and based on these results some bacterial species can be seen to be consistently present throughout the biodegradation. Band numbers increased from 9 in the chemostat (data not shown) to 18 in sample NW0, which is when there was an adequate supply of PYR (1992 mg/kg) as the sole carbon source in the batch reactor. There were usually more free-living bacterial species than soil particle-attached bacterial species in the same sample from the ABR, except for samples NW5 and NS5. For example, the number of DGGE bands in the NW samples ranged from 18 to 20, which is greater than the range 13 to 19 present in the SW samples. Some bacterial species known to be involved in PYR biodegradation were located as forming bands NB5, NB6, and NB7 in the NW and SW samples. The bacteria encoding bands NB8 and NB9 were present in the SW samples only.

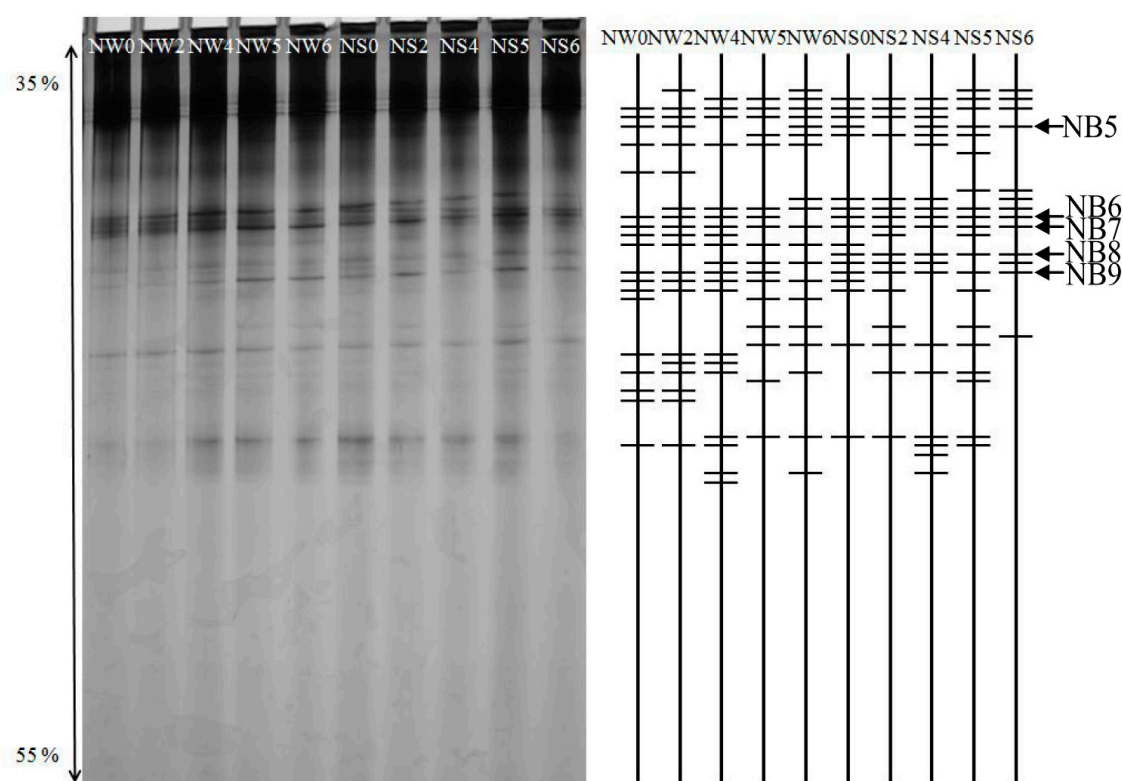


Figure 3. DGGE profiles during PYR biodegradation in an ABR. NW, Free-living bacteria; NS, Soil-attached bacteria; NW-X or NS-X, X = 0, 2, 4, 5, 6 represent the biodegradation samples at 0, 14, 28, 35, 42 days, respectively. NB5, NB6, NB7, NB8 and NB9 represent commonly occurring bacterial species.

Figure 4 shows the differences between free-living bacterial community and soil particle-attached bacterial community during PYR biodegradation in the ABR. *Pseudomonas*, *Rhodanobacter*, and *Acinetobacter* were dominant in the NW samples. On the other hand, the soil particle-attached bacterial species consisted largely of green sulfur bacteria, *Sphingomonas*, *Rhodanobacter*, *Pseudomonas*, *Chlorobi*, *Verrucomicrobia*, *Acidobacteria*, *Gemmatimonas*, and *Planctomycete*. Table 4 shows the variations in bacterial species that occurred over the time course of the PYR biodegradation in the ABR. Eleven bacterial species in total were found in the batch reactor (N2000). *Rhodanobacter*, *Mycobacterium*, *Geobacter*, *Delftia*, *Acidobacteria*, green sulfur bacteria, *Chlorobi*, *Ignavibacterium*, *Verrucomicrobia*, *Gemmatimonas*, and *Planctomycete* were identified in the N2000 sample. Nine bacterial species in total were found in the NW samples and five of the nine species were the same as those in the N2000 sample. The four extra bacterial species that were detected consisted of *Acinetobacter*, *Pseudomonas*, *Caulobacter*, and *Cryobacterium mesophilum*. Moreover, eleven bacterial species were detected in the NS samples and seven of these bacterial species were the same as those in the N2000 sample. The extra bacterial species consisted of *Acinetobacter*, *Pseudomonas*, *Sphingomonas*, and *Burkholderia*. Six of the fourteen bacterial species in the NW and NS samples, namely Green sulfur bacteria, *Mycobacterium*, *Verrucomicrobium*, *Acidobacteria*, *Acinetobacter*, and *Pseudomonas* were detected as being present in both samples at the same time point.

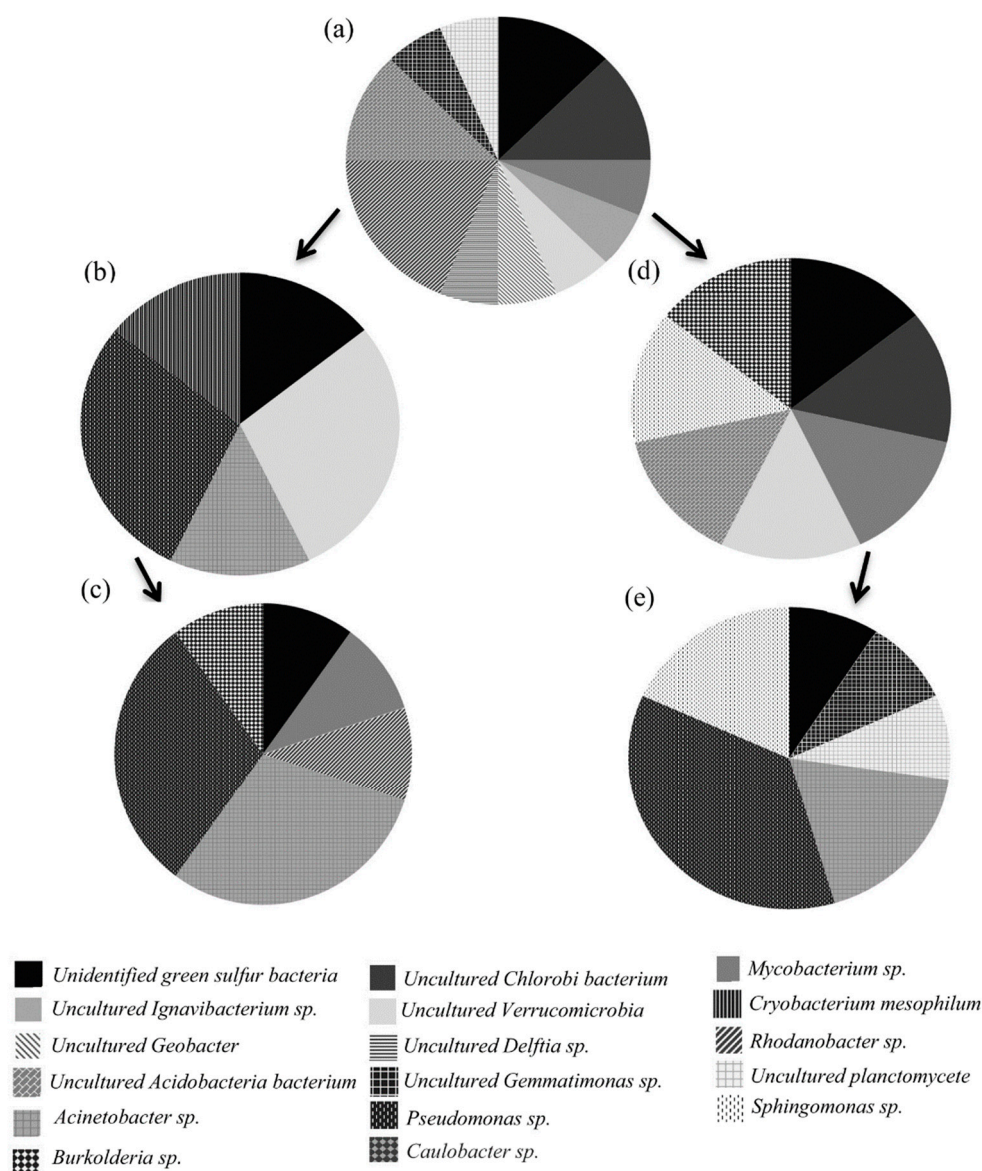


Figure 4. Changes in the bacterial community present during PYR biodegradation in an ABR. NW, Free-living bacteria; NS, Soil-attached bacteria; NW-X or NS-X, X = 5, 6 represent the biodegradation samples at 35, 42 days, respectively: (a) Chemostat N; (b) NW5; (c) NW6; (d) NS5; (e) NS6.

Table 4. Bacteria identified by nucleic acid sequencing of 16S rDNA gene clones and by searching the GenBank database; these are believed to be associated with the biodegradation of PYR and various aromatic compounds in the ABR.

Bacterial Species	NCBI Accession No. (Closest Match)	Sequences Similarity (%)	Samples ¹		
			N2000	NW	NS
Green sulfur bacterium	AJ630296	99	+	+	+
Chlorobi bacterium	EF446837	98	+	–	+
<i>Mycobacterium</i> sp.	AJ783967	99	+	+	+
<i>Ignavibacterium</i> sp.	JQ724348	85	+	–	–
Verrucomicrobia bacterium	DQ450782	95	+	+	+
<i>Geobacter</i> sp.	AM712168	100	+	–	–

Table 4. Cont.

Bacterial Species	NCBI Accession No. (Closest Match)	Sequences Similarity (%)	Samples ¹		
			N2000	NW	NS
<i>Delftia</i> sp.	FN435935	92	+	–	–
<i>Rhodanobacter</i> sp.	FJ608778	100	+	+	–
<i>Acidobacteria</i> bacterium	FJ535087	99	+	+	+
<i>Gemmatimonas</i> sp.	EU283563	96	+	–	+
Planctomycete bacterium	JN038656	94	+	–	+
<i>Acinetobacter</i> sp.	JF901932	100	–	+	+
<i>Pseudomonas</i> sp.	AM911668	100	–	+	+
<i>Sphingomonas</i> sp.	AB235162	98	–	–	+
<i>Burkholderia</i> sp.	DQ279344	97	–	–	+
<i>Caulobacter</i> sp.	JF905609	99	–	+	–
<i>Cryobacterium mesophilum</i>	NR044239	99	–	+	–

¹ +: Positive; –: Negative.

3.3. Functional Genes Present During PYR Biodegradation

A number of genes encoding dioxygenases, which are highly relevant to PYR biodegradation, were able to be amplified from the ABR genomic DNA samples. Table 5 shows the presence of these various genes in free-living bacteria and soil particle-attached bacteria. Positive signals for various dioxygenases, including RHD α , Rf and C23O, were identified in both free-living bacteria and soil particle-attached bacteria (see the Supplementary Figure S2). However, DNA encoding P34O was only detected by PCR as being presented as the initial inoculum from the chemostat N and in the batch reactor sample (N2000). Genes encoding NidA were not detected by PCR and this would not seem to be present during PYR biodegradation in the ABR.

Table 5. Presence of dioxygenases during PYR biodegradation.

Primer Sample ¹	RHD α	Nid A	Rf	P340	C230
Chemostat N	+	–	+	+	+
N2000	+	–	+	+	+
NW0/NS0	+/+	–/–	+/+	–/–	+/+
NW2/NS2	+/+	–/–	+/+	–/–	+/+
NW4/NS4	+/+	–/–	+/+	–/–	+/+
NW5/NS5	+/+	–/–	+/+	–/–	+/+
NW6/NS6	+/+	–/–	+/+	–/–	+/+

¹ NW-X or NS-X, X = 0, 2, 4, 5, 6 present the biodegradation samples at 0, 14, 28, 35, 42 days, respectively.

3.4. CLPP

CLPP, using average well color development, was explored using principal component analysis (PCA). Each point on the CLPP represents a BioLog Ecoplate pattern and the distances between points approximate to pattern similarity. Figure 5 shows the CLPPs for PYR biodegradation in the ABR free-living bacteria and soil particle-attached bacteria have very different CLPP plots. Free-living bacteria show an obvious diversity on the CLPP plot, which probably represents the bacterial occurrence of PYR biodegradation in the NW samples. No significant change in the NS samples was found during PYR biodegradation. This result implies that the physiological characteristics in the ABR of free-living bacteria involving in the biodegradation of PYR are very different to those of the soil particle-attached bacteria, which would seem to be somewhat less involved in the biodegradation of PYR. However, the CLPP is not able to be directly related to the variations

detected in free-living and particle-base bacterial communities in the ABR. Nevertheless, the species distribution within the two bacterial communities in the ABR may play very important, but probably different roles in the physiological characteristics of the ABR.

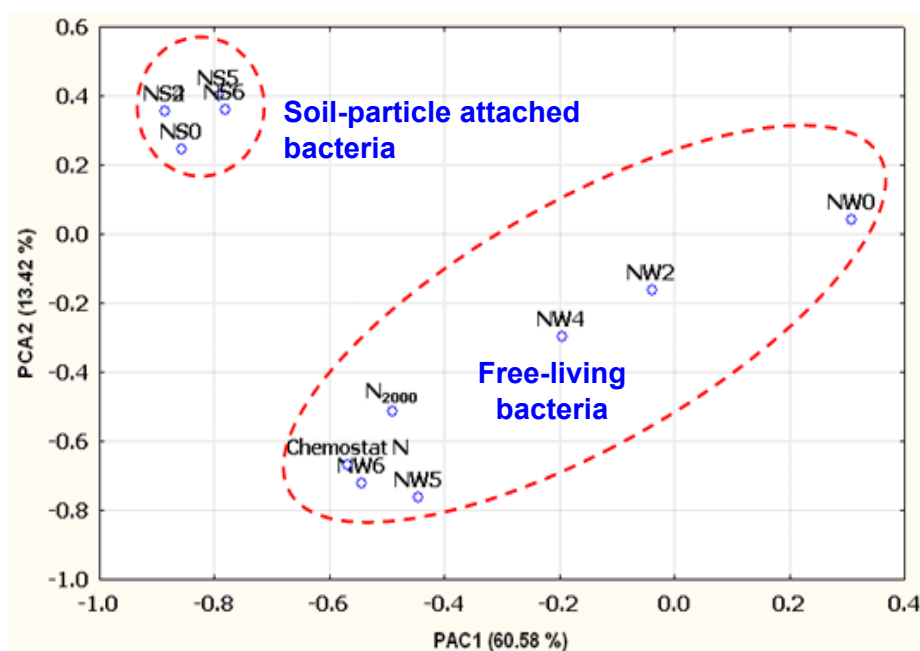


Figure 5. A community level physiological profiling (CLPP) plot of the first (PAC1) and the second (PAC2) principal components of the PYR biodegradation in an ABR (PAC1 + PAC2 = 74%). Chemostat N and N2000: See Section 2.1 NW = Free-living bacteria; NS = Soil-attached bacteria. 0, 2, 4, 5, 6 represent the biodegradation samples at 0, 14, 28, 35, 42 days, respectively.

4. Discussion

4.1. The bacterial Species Identified as Present During the PYR Biodegradation in the ABR

Free-living bacteria seem to play an important role in PYR biodegradation in the studied ABR soil/water system. The dominant bacteria involved in PYR biodegradation in the ABR were identified. Previously, a free-living *Sphingomonas* has been identified as having the ability of biodegrading PYR [21]. Similarly, a *Burkholderia* has been reported to have the ability to biodegrade MHW PAHs, including dibenz[a,h]anthracene, benz[a]anthracene, fluoranthene and PYR. Furthermore, *Pseudomonas putida* isolates are known to be able to biodegrade PYR in soil environments [22,23] and *Mycobacterium* spp. are commonly present during PAHs-contaminated soil bioremediation, and they are able to utilize HMW PAHs as their sole carbon and energy source [24,25]. In addition, *Rhodanobacter lindaniclasticus* is able to degrade MHW PAHs, such as benzo[a]pyrene [26] and a *Verrucomicrobia* sp. is known to be present in soil and is able to degrade carbonates [27]. Finally, a *Geobacter* sp. is known to degrade many aromatic compounds, including 4-hydroxybenzaldehyde, benzaldehyde and benzoate [28], and a *Delftia* sp., that was isolated from a mixture culture of PAHs-biodegraders was shown to be able to degrade humic acid-sorbed phenanthrene [29]. Other bacterial species have also been identified as being likely to be able to help with PYR bioremediation indirectly in the ABR. For example, green sulfur bacteria are chemotrophic bacteria and are able to utilize carbon dioxide as the carbon source and release oxygen into the micro environment of the slurry soil [30]. Furthermore, *Planctomycetales* strains, members of the anammox group of bacteria, are known to be involved in the anammox process in ABRs containing micro-anaerobic soil slurry [31]. Finally, a decrease in a *Chlorobi* spp. from 5.3% to 0.7% has been found under anoxic nitrate reducing conditions when there are PAH-induced changes in mud activated sludge from a biological wastewater treatment process [32].

4.2. Comparison of Biodiversity of Free-Living Bacteria and Soil-Particle Bacteria Present in the ABR During PYR Bioremediation

Microbial biodiversity during PYR bioremediation in the ABR can be presented in three different ways; namely by a Shannon Weaver Index (SWI), by species Richness (R) and by species Evenness (E). The Richness (R) values are calculated using the number of DNA bands detected in the various DGGE profiles. The SWI and E values are calculated using DGGE band numbers and DGGE band density [33]. Table 6 shows the SWI index trend is similar to the change of DGGE band numbers. In addition, at the beginning of experiment, the SWI of NW0 (1.10) was almost the same as that of SW0 (1.09); and from that point onwards the SWI values are always “aqueous state > soil particle-attached state” during the PYR bioremediation in the ABR, For example, 1.18 (NW2) > 1.06 (NS2); 1.18 (NW4) > 1.13 (NS4); 1.03 (NW5) > 0.87 (NS5); 1.08 (NW6) > 0.90 (NS6). Moreover, the biodiversity of both free-living bacteria and soil particle-attached bacteria show an increasing trend from low to high from the start of PYR biodegradation. One possible reason for this is that, with PYR as a sole carbon source, the biodegradation involves only a single compound that is then converted into a variety of different biometabolites during the ABR process. These new biometabolites then provide a wider variety of carbon sources, each of which can now be utilized by various different bacterial species. Supporting this, the SWI indices can be seen to increase from 1.10 at NW0 to 1.18 at NW4 and from 1.09 at NS0 to 1.13 at NS4. When these biometabolites are used up, the biodiversity of the bacteria in the ABR begins to decrease; thus the SWI values then drop from 1.18 (NW4) to 1.08 (NW6) and from 1.13 (NS4) to 0.90 (NS6). If we examine the R and E indices, there are similar trends to that of the SWI values as PYR biodegradation progresses in the ABR.

Table 6. Variations in Shannon Weaver Index (SWI), Richness (R) and Evenness (E) of bacterial diversity during PYR biodegradation. NW samples represent free-living bacteria. NS samples represent soil particle-attached bacteria.

NW ¹	Biodiversity			NS ¹	Biodiversity		
	SWI	R	E		SWI	R	E
N ₂₀₀₀	0.84	9	0.38	-	-	-	-
NW0	1.10	18	0.37	NS0	1.09	17	0.38
NW2	1.18	20	0.39	NS2	1.06	17	0.36
NW4	1.18	20	0.42	NS4	1.13	19	0.38
NW5	1.03	17	0.35	NS5	0.87	20	0.34
NW6	1.08	19	0.38	NS6	0.90	13	0.31

¹ NW-X or NS-X, X = 0, 2, 4, 5, 6 present the biodegradation samples at 0, 14, 28, 35, 42 days, respectively.

4.3. The Presence of Dioxygenases as Functional Genes During PYR Biodegradation in the ABR

The dioxygenases produced by PAHs-biodegrading bacteria are able to cleave the fused benzene structure of PYR. Figure 6 shows the integrated pathway of PYR biodegradation predicted using the biometabolites detected in this study and the fact that dioxygenases are present. The integrated pathway of PYR biodegradation with selective dioxygenases in this study can be summarized as including the following: (1) The presence of typical PYR-biodegraders, including *Mycobacterium flavescens*, *Mycobacterium* spp. AP1, KR2, 6PY1, *Mycobacterium vanbaalenii* PYR-1, *Pseudomonas stutzeri* P16, *Bacillus cereus* P21 [34,35] and (2) the presence of the dioxygenases RHD α , Rf, C23O, P34O [12,14,36]. The hydrophilicity of the metabolites of PYR is higher than that of PYR itself and they are thus able to easily dissolve in the aqueous phase; this is because they have OH functional groups or similar present [37,38]. PYR biodegradation in the batch reactor (N2000) involves a number of bacterial species (see Figure 4) and this means that there are two possible metabolic pathways that involve the four target dioxygenases, RHD α , Rf, P34O and C23O. However, a decrease in bacterial species was found

in the ABR and as a result only a single metabolic pathway seems to be present based on the fact that there were reduced positive responses for three of the target dioxygenases (RHD α , Rf and C23O).

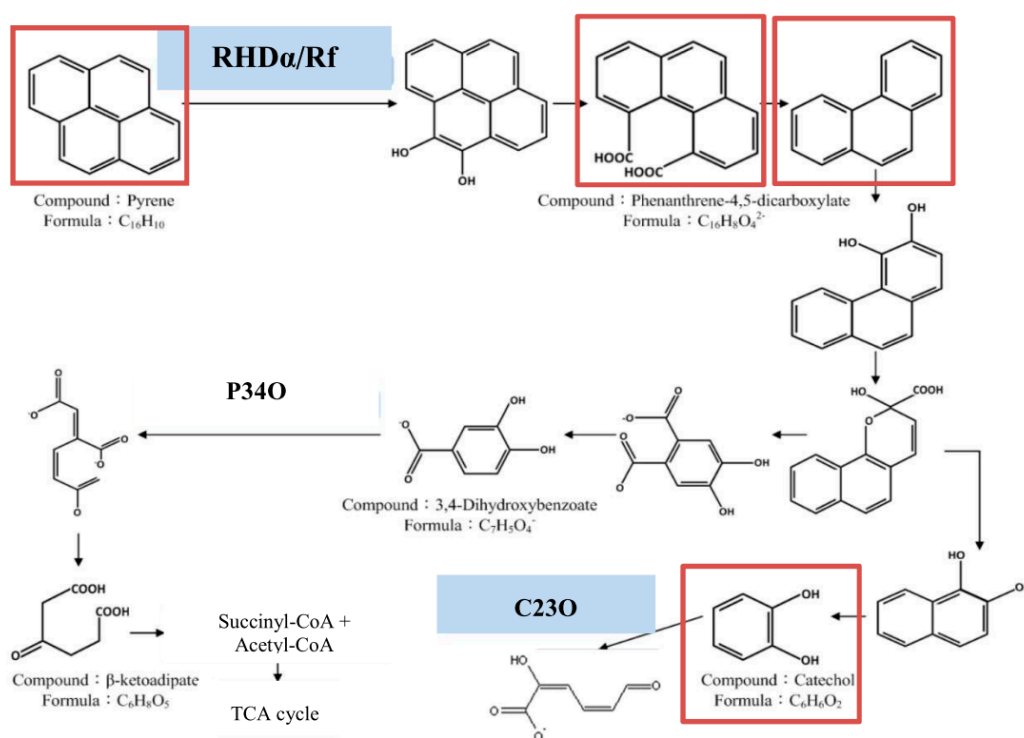


Figure 6. The integrated pathway for PYR biodegradation based on the positive responses for the presence of the target dioxygenases in the ABR [12,14,34–36]. Biometabolites marked brown were identified by GC-MS in this study. The various target dioxygenases marked in blue have been positively detected in this study.

PAH RHD α is a component of the RHD enzyme system that consists of three components, these are an iron-sulfur flavoprotein reductase, which is followed by an iron-sulfur ferredoxin transfer of electrons from NAD(P)H to a terminal dioxygenase [39]. The terminal dioxygenase is able to catalyze the degradation of PAHs via its active site a series of electron transportation events. The enzyme demonstrates a high level of conservation across various different microorganisms. Under aerobic conditions, this initial step commonly occurs via the incorporation of molecular oxygen into an aromatic nucleus via the multicomponent RHD enzyme system; this forms cis-dihydrodiol. This gene complex can be an excellent indicator that is able to help our understanding of the potential bioavailability of aromatic compounds and has allowed the horizontal gene transfer of these genes to be traced in a bacterial community [40–42].

The Rf genes encode the larger α -subunit of a terminal dioxygenase; this gene has been used as an oxygenase indicator when there is aromatic substrate specificity and when the dioxygenase is the rate-limiting step. The α -subunit amplified here is the catalytic component and contains two conserved regions: The [Fe₂-S₂] Risaker center and the mononuclear iron binding domain. These two centers are involved in consecutive electron transfer to a dioxygen molecule.

C23O, which is a member of the extradiol dioxygenase family and catalyzes the *meta*-cleavage of catechol, methyl-substituted catechol and ethyl-substituted catechol; such cleavages play important roles in the later steps of the degradation pathways of hydrogen aromatic compounds. A wide variety of C23O genes from identified bacterial species have been found in ABR systems that are involved in the biodegradation of PAHs. For example, the expression of C23O in *Burkholderia cepacia* has been shown to be responsible for the degradation of PYR and to play an important role in improving the biodegradation of PYR [43]. C23O enzyme activity has been detected in a bioaugmented soil

microcosm where PYR has been added at $61.80 \pm 2.20 \text{ nmol min}^{-1} \text{ mg}^{-1}$ protein. The soil microcosm with added PYR was able to show the presence of both the catechol and phthalate pathways during PYR degradation [44].

Nid A and P34O seem to be absent during PYR biodegradation in our ABR based on the PCR results. The Nid A gene encodes the α -NidA polypeptide of the terminal dioxygenase and was originally cloned from *Mycobacterium vanbaalenii* strain PYR-1 isolated from a petrogenic chemical-pollution site [16]. One other possible reason for the negative PCR result is that the primers used may be too species specific and thus unable to target dioxygenases from a wide range of bacterial species. Genes encoding P34O were only detected as present by PCR in the initial inoculum (N2000) sample and in the chemostat used for PYR biodegradation. Various possible reasons for this absence once the ABR system starts bioremediation can be suggested and these include: (1) The para-cleavage of PAHs during biodegradation is significantly limited in the ABR, but does occur extensively in the chemostat and in the initial inoculum; and (2) it should be noted that *Bacillus* spp. and *Sphingomonas* spp. known to be involved in the biodegrading of biometabolite 3,4-dihydroxybenzoic acid by C34O were not identified in an earlier ABR system [40] and this also seems to be the case here.

5. Conclusions

The high-level concentration of HMW PAHs (PYR)-contaminated soil can be biodegraded effectively by a mixture culture enriched with PYR-biodegraders. The major function of free-living bacteria and soil-particle bacteria during PYR biodegradation in the ABR are outlined here in detail. Free-living bacteria play an important role in the biodegradation of PYR in the ABR. *Mycobacterium* spp., *Pseudomonas putida* and *Burkholderia* spp. were identified as present during the PYR biodegradation. Larger amounts of biometabolites from PYR are able to be detected at the one time point, when there is very high biodiversity of free-living bacteria present in the ABR. The PYR biodegradation pathways seem to involve the rieske nonheme iron aromatic ring-hydroxylating dioxygenase, the α subunit of the rieske iron-sulfur dioxygenase and catechol 2,3-dioxygenase. Greater utilization of the available carbon sources by free-living bacteria than by soil-bound bacteria was detected by CLPP plot and it is possible that the soil particle-attached bacteria may not be directly involved in PYR biodegradation, but they do seem to help with the breakdown of some of the biological products created during the PYR ecological cycle. The experimental results presented in this study will help with designing POP bioremediation systems using ABRs. The detection of various dioxygenase genes, such as RHD α , Rf and C23O, could be a useful indicator when evaluating the effective removal of HMW PAHs or other aromatic compounds during biodegradation.

Supplementary Materials: The following are available online at <http://www.mdpi.com/2071-1050/11/4/1088/s1>, Figure S1: Biometabolites identified by GC-MS. AW = aqueous samples; NS = soil-attached samples; N2 present the biodegradation samples at the 14 day. (a) phenanthrene; (b) catechol; (c) dibenzothiophene; (d) 4-Carboxy-5-phenanthrenecarboxaldehyde; (e) cyclopentaphenanthren; (f) 4,4'-Bipyrimidine. Figure S2: Responses to dioxygenases encoding target functional genes in PYR biodegradation in the ABR.

Author Contributions: Conceptualization, Y.-T.C. and C.-C.Y.; Methodology, C.-C.Y. and Y.-T.C.; Software, C.-C.Y. and T.-C.C.; Investigation, C.-C.Y.; Resources, Y.-T.C.; Data curation, C.-C.Y. and T.-C.C.; Writing—original draft preparation, C.-C.Y. and Y.-T.C.; Writing—review and editing, Y.-T.C. and C.-S.L.

Funding: This work was supported by the MOST projects: NSC98-2221-E-031 and MOST104-2221-E-031-001-MY2. Part of the results/discussion was presented at the 7th International Conference on Challenges in Environmental Science & Engineering (CESE-2014) in 2014 and the 10th International Conference on Challenges in Environmental Science & Engineering (CESE-2017) in 2017.

Conflicts of Interest: The authors declare no conflict of interest.

References

1. Lawal, A.T. Polycyclic aromatic hydrocarbons: A review. *Cogent Environ. Sci.* **2017**, *3*, 1339841. [[CrossRef](#)]

2. Machin-Ramirez, C.; Okoh, A.I.; Morales, D.; Mayolo-Deloisa, K.; Quintero, R.; Trejo-Hernández, M.R. Slurry-phase biodegradation of weathered oily sludge waste. *Chemosphere* **2008**, *70*, 737–744. [[CrossRef](#)] [[PubMed](#)]
3. Mohan, S.V.; Prasanna, D.; Reddy, B.P.; Sarma, P.N. Ex situ bioremediation of pyrene contaminated soil in bioslurry phase reactor operated in periodic discontinuous batch mode: Influence of bioaugmentation. *Int. Biodeterior. Biodegrad.* **2008**, *62*, 162–169. [[CrossRef](#)]
4. Pavel, L.V.; Gavrilesco, M. Overview of Ex Situ decontamination techniques for soil cleanup. *Environ. Eng. Manag. J.* **2008**, *7*, 815–834. [[CrossRef](#)]
5. Nasser, S.; Kalantary, R.R.; Nourieh, N.; Naddafi, K.; Mahvi, A.H.; Baradaran, N. Influence of bioaugmentation in biodegradation of PAHs-contaminated soil in bio-slurry phase reactor. *Iran. J. Environ. Health Sci. Eng.* **2010**, *7*, 199–208.
6. Robles-González, I.; Ríos-Leal, E.; Ferrera-Cerrato, R.; Esparza-García, F.; Rinderknecht-Seijas, N.; Poggi-Varaldo, H.M. Bioremediation of a mineral soil with high contents of clay and organic matter contaminated with herbicide 2,4-dichlorophenoxyacetic acid using slurry bioreactors: Effect of electron acceptor and supplementation with an organic carbon source. *Process Biochem.* **2006**, *41*, 1951–1960. [[CrossRef](#)]
7. Ghosal, D.; Ghosh, S.; Dutta, T.K.; Ahn, Y. Current state of knowledge in microbial degradation of polycyclic aromatic hydrocarbons (PAHs): A review. *Front. Microbiol.* **2016**, *7*, 1369. [[CrossRef](#)]
8. Chang, Y.-T.; Lee, J.-F.; Chao, H.-P.; Liao, W.-L. Bacterial community changes with N'-N' dimethylformamide (DMF) additives during polycyclic aromatic hydrocarbons (PAH) biodegradation. *Environ. Technol.* **2010**, *27*, 1–14. [[CrossRef](#)]
9. Chang, Y.-T.; Chou, H.-L.; Chao, H.-P.; Chang, Y.-J. The influence of sorption on polyaromatic hydrocarbon biodegradation in the presence of modified nonionic surfactant organoclays. *Int. Biodeterior. Biodegrad.* **2015**, *102*, 237–244. [[CrossRef](#)]
10. Mohan, S.V.; Kisa, T.; Ohkuma, T.; Kanaly, R.A.; Shimizu, Y. Bioremediation technologies for treatment of PAH-contaminated soil and strategies to enhance process efficiency. *Rev. Environ. Sci. Biotechnol.* **2006**, *5*, 347–374. [[CrossRef](#)]
11. Painter, R.D.; Kochary, S.; Byl, T.D. Free-living bacteria or attached bacteria: Which contributes more to bioremediation? In *U.S. Geological Survey Karst Interest Group Proceedings*; US Geological Survey Karst Interest Group: Rapid City, SD, USA, 2005.
12. Ding, G.C.; Heuer, H.; Zühlke, S.; Spitteller, M.; Pronk, G.J.; Heister, K.; Kögel-Knabner, I.; Smalla, K. The diversity and abundance of PAHs-ring hydroxylating dioxygenase genes studied by a novel PCR detection system revealed soil type dependent responses to phenanthrene. *Appl. Environ. Microbiol.* **2010**, *76*, 4765–4771. [[CrossRef](#)] [[PubMed](#)]
13. Kumar, A.; Kumar, S.; Kumar, S. Biodegradation kinetics of phenol and catechol using *Pseudomonas putida* MTCC 1194. *Biochem. Eng. J.* **2005**, *22*, 151–159. [[CrossRef](#)]
14. Iwagami, G.S.; Yang, K.; Davies, J. Characterization of the protocatechuic acid catabolic gene cluster from *Streptomyces* sp. strain 2065. *Appl. Environ. Microbiol.* **2000**, *66*, 1499–1508. [[CrossRef](#)] [[PubMed](#)]
15. Alfreider, A.; Vogt, C.; Babel, W. Expression of chlorocatechol 1,2-dioxygenase and chlorocatechol 2,3-dioxygenase genes in chlorobenzene-contaminated subsurface samples. *Appl. Environ. Microbiol.* **2003**, *69*, 1372–1376. [[CrossRef](#)] [[PubMed](#)]
16. Brezna, B.; Khan, A.A.; Cerniglia, C.E. Molecular characterization of dioxygenases from polycyclic aromatic hydrocarbon-degrading *Mycobacterium* spp. *FEMS Microbiol. Lett.* **2003**, *233*, 177–183. [[CrossRef](#)]
17. Liu, B.; Li, Y.; Zhang, X.; Wang, J.; Gao, M. Effects of chlortetracycline on soil microbial communities: Comparisons of enzyme activities to the functional diversity via Biolog EcoPlates™. *Eur. J. Soil Biol.* **2015**, *68*, 69–76. [[CrossRef](#)]
18. Lladó, S.; Baldrian, P. Community-level physiological profiling analyses show potential to identify the copiotrophic bacteria present in soil environments. *PLoS ONE* **2017**, *12*, e0171638. [[CrossRef](#)] [[PubMed](#)]
19. Chou, H.-L.; Hwa, M.-Y.; Lee, Y.-C.; Chang, Y.-J.; Chang, Y.-T. Microbial degradation of decabromodiphenyl ether (DBDE) in soil slurry microcosms. *Environ. Sci. Pollut. Res. Int.* **2016**, *23*, 5255–5267. [[CrossRef](#)]
20. Guha, S.; Peters, C.A.; Jaffé, P.R. Multisubstrate biodegradation kinetics of naphthalene, phenanthrene, and pyrene mixtures. *Biotechnol. Bioeng.* **1999**, *65*, 491–499. [[CrossRef](#)]

21. Herwijnen, V.R.; Wattiau, P.; Batiaens, L.; Daai, L.; Jonker, L.; Springaei, D.; Govers, H.A.J.; Parsons, J.R. Elucidation of the metabolic pathway of fluorine and cometabolic pathways of phenanthrene, fluoroanthene, anthracene and dibenzothiophene by *Sphingomonas* sp. LB126. *Res. Microbiol.* **2003**, *154*, 199–206. [[CrossRef](#)]
22. Juhasz, L.A.; Britz, M.L.; Stanley, G.A. Degradation of fluoranthene, pyrene, benz[a]anthracene and dibenz[a,h]anthracene by *Burkholderia cepacia*. *J. Appl. Microbiol.* **1997**, *83*, 189–198. [[CrossRef](#)]
23. O'Sullivan, A.L.; Mahenthalingam, E. Biotechnological potential within the genus *Burkholderia*. *Let. Appl. Microbiol.* **2005**, *41*, 8–11. [[CrossRef](#)] [[PubMed](#)]
24. Kim, R.J.; Min, B.; Logan, B.E. Evaluation of procedures to acclimate a microbial fuel cell for electricity production. *Appl. Microbiol. Biotechnol.* **2005**, *68*, 23–30. [[CrossRef](#)]
25. Uytendroek, M.; Vermeir, S.; Wattiau, P.; Ryngaert, A.; Springael, D. Characterization of cultures enriched from acidic polycyclic aromatic hydrocarbon-contaminated soil for growth on pyrene at low pH. *Appl. Environ. Microbiol.* **2007**, *73*, 3159–3164. [[CrossRef](#)] [[PubMed](#)]
26. Kanaly, A.R.; Harayama, S.; Watanabe, K. *Rhodanobacter* sp. Strain BPC1 in a benzo[a]pyrene-mineralizing bacterial consortium. *Appl. Environ. Microbiol.* **2002**, *68*, 5826–5833. [[CrossRef](#)]
27. Zhang, L.; Xu, Z. Assessing bacterial diversity in soil. *J. Soils Sediments* **2008**, *8*, 379–388. [[CrossRef](#)]
28. Butler, J.E.; He, Q.; Nevin, K.P.; He, Z.; Zhou, J.; Lovley, D.R. Genomic and microarray analysis of aromatics degradation in *Geobacter metallireducens* and comparison to a *Geobacter* isolate from a contaminated field site. *BMC Genom.* **2007**, *8*, 180. [[CrossRef](#)]
29. Vacca, D.J.; Bleam, W.F.; Hickey, W.J. Isolation of soil bacteria adapted to degrade humic acid-sorbed phenanthrene. *Appl. Environ. Microbiol.* **2005**, *71*, 3797–3805. [[CrossRef](#)]
30. Imhoff, J.F. Taxonomy and physiology of phototrophic purple bacteria and green sulfur bacteria. In *Anoxygenic Photosynthetic Bacteria. Advances in Photosynthesis and Respiration*; Blankenship, R.E., Madigan, M.T., Bauer, C.E., Eds.; Springer: Dordrecht, The Netherlands, 1995; Volume 2, pp. 1–15, ISBN 978-0-306-47954-0.
31. Tai, Y.; Watts, J.E.M.; Schreier, H.J. Anaerobic ammonium-oxidizing (Anammox) bacteria and associated activity in fixed-film biofilters of a marine recirculating aquaculture system. *Appl. Environ. Microbiol.* **2006**, *72*, 2896–2904.
32. Martirani-Von Abercron, S.-M.; Pacheco, D.; Benito-Santano, P.; Marín, P.; Marqués, S. Polycyclic aromatic hydrocarbon-induced changes in bacterial community structure under anoxic nitrate reducing conditions. *Front. Microbiol.* **2016**, *7*, 1775. [[CrossRef](#)]
33. Dong, X.; Reddy, G.B. Soil bacterial communities in constructed wetlands treated with swine wastewater using PCR-DGGE technique. *Bioresour Technol.* **2010**, *101*, 1175–1182. [[CrossRef](#)] [[PubMed](#)]
34. Seo, J.S.; Keum, Y.S.; Li, Q.X. Bacterial degradation of aromatic compounds. *Int. J. Environ. Res. Public Health* **2009**, *6*, 278–309. [[CrossRef](#)] [[PubMed](#)]
35. Kweon, O.; Kim, S.J.; Cerniglia, C.E. Genomic view of Mycobacterial high molecular weight polycyclic aromatic hydrocarbon degradation. In *Handbook of Hydrocarbon and Lipid Microbiology*; Timmis, K.N., McGenity, T.J., van der Meer, J.R., de Lorenzo, V., Eds.; Springer: Berlin/Heidelberg, Germany, 2010; pp. 1166–1175, ISBN 978-3-540-77588-1.
36. Mesarch, B.M.; Nakatsu, C.H.; Nies, L. Development of catechol 2,3-dioxygenase-specific primers for monitoring bioremediation by competitive quantitative PCR. *Appl. Environ. Microbiol.* **2000**, *66*, 678–683. [[CrossRef](#)]
37. Arora, K.P.; Kumar, M.; Chauhan, A.; Raghava, G.P.S.; Jain, R.K. OxDbase: A database of oxygenases involved in biodegradation. *BMC Res. Notes* **2009**, *2*, 1–8. [[CrossRef](#)]
38. Gao, J.E.; Lynda, M.B.; Wackett, L.P. The university of minnesota biocatalysis/biodegradation database: Improving public access. *Nucleic Acids Res.* **2010**, *38*, D488–D491. [[CrossRef](#)]
39. Lyu, Y.; Zheng, W.; Zheng, T.; Tian, Y. Biodegradation of polycyclic aromatic hydrocarbons by *Novosphingobium pentaromativorans* US6-1. *PLoS ONE* **2014**, *9*, e101438. [[CrossRef](#)]
40. Moser, R.; Stahl, U. Insights into the genetic diversity of initial dioxygenases from PAH-degrading bacteria. *Appl. Microbiol. Biotechnol.* **2001**, *55*, 609–618. [[CrossRef](#)]
41. Dutta, C.; Pan, A. Horizontal gene transfer and bacterial diversity. *J. Biosci.* **2002**, *27*, 27–33. [[CrossRef](#)]

42. Mercier, A.; Kay, E.; Simonet, P. Horizontal Gene Transfer by Natural Transformation in Soil Environment. In *Nucleic Acids and Proteins in Soil. Soil Biology*; Nannipieri, P., Smalla, K., Eds.; Springer: Berlin/Heidelberg, Germany, 2006; Volume 8, pp. 355–373. ISBN 978-3-540-29448-1.
43. Chen, K.; Zhu, Q.; Qian, Y.; Song, Y.; Yao, J.; Choi, M.M. Microcalorimetric investigation of the effect of non-ionic surfactant on biodegradation of pyrene by PAH-degrading bacteria *Burkholderia cepacia*. *Ecotoxicol. Environ. Saf.* **2013**, *98*, 361–367. [[CrossRef](#)]
44. Mangwani, N.; Kumari, S.; Das, S. Marine bacterial biofilms in bioremediation of polycyclic aromatic hydrocarbons (PAHs) under terrestrial condition in a soil microcosm. *Pedosphere* **2017**, *27*, 548–558. [[CrossRef](#)]



© 2019 by the authors. Licensee MDPI, Basel, Switzerland. This article is an open access article distributed under the terms and conditions of the Creative Commons Attribution (CC BY) license (<http://creativecommons.org/licenses/by/4.0/>).